Acta Crystallographica Section B
Structural Science
ISSN 0108-7681

Structural stability and formability of ABO_3-type perovskite compounds

Huan Zhang, Na Li, Keyan Li and Dongfeng Xue*

State Key Laboratory of Fine Chemicals, Department of Materials Science and Chemical Engineering, Dalian University of Technology, Dalian 116012, People's Republic of China

Correspondence e-mail: dfxue@chem.dlut.edu.cn

Received 22 May 2007
Accepted 20 September 2007

On the basis of the bond-valence model (BVM) and structure-map technology, the structural stability and formability of ABO_3-type perovskite compounds were investigated in 376 ABO_3-type compounds. A new criterion of structural stability for ABO_3-type perovskite compounds has been established by the bond-valence calculated tolerance factors, which are in the range 0.822−1.139. All global instability indices for ABO_3-type perovskite compounds are found to be less than 1.2 v.u. (valence units) and increase with a decrease in oxidation state of the B cations (*i.e.* structural stability in the formation of an ideal cubic perovskite follows the order $A^{+}B^{5+}O_3$-type > $A^{2+}B^{4+}O_3$-type > $A^{3+}B^{3+}O_3$-type). Three new two-dimensional structure maps were constructed based on the ideal $A-O$ and $B-O$ bond distances derived from the BVM. These maps indicate the likelihood of particular perovskite compounds being formed. The present work enables novel perovskite and perovskite-related compounds to be explored by screening all the possible elemental combinations in future crystal engineering.

1. Introduction

The perovskite structure is one of the most frequently encountered structure types in solid-state inorganic chemistry. It accommodates cations of most of the metallic elements in the periodic table and a significant number of anions. Although most of the compounds that adopt the perovskite structure are oxides and fluorides, some hydrides (Sato *et al.*, 2005), oxyfluorides (Alekseeva *et al.*, 2004) and oxynitrides (Rooke & Weller, 2003) are also found to crystallize in this structure. Structurally, the ideal perovskite oxide has a stoichiometry formula of ABO_3 and belongs to the cubic space group $Pm\bar{3}m$ (No. 221), with the A cation in a 12-fold coordination site and the B cation in a sixfold coordination site. As shown in Fig. 1, the A cation is located at the body center of the cube, the B cation is at each of the eight corners and the O anion is at each of the centers of the 12 edges. The most common description of a perovskite structure is a three-dimensional framework of corner-sharing BO_6 octahedra, with the A cation filling the 12-coordinate cavities.

Owing to the non-stoichiometry of the cation or anion, the distortion of the cation configuration and the electronic structure arising from mixed-valence, perovskite and perovskite-related materials exhibit versatile physical and chemical properties, which have attracted considerable research interest in materials chemistry. For instance, perovskite ceramics with ferroelectric and piezoelectric properties, such as $BaTiO_3$, $PbTiO_3$, Bi_2ZnTiO_6 (Suchomel *et al.*, 2006) and $Bi(Mg_{1/2}Ti_{1/2})O_3$ (Khalyavin *et al.*, 2006) play a dominant role in the electroceramics industry. Other industrial applications

of perovskites are: catalysis ($LaFeO_3$; De & Barresi, 2001), ion conduction ($LaGaO_3$; Kajitani *et al.*, 2005), linear and nonlinear optical switching ($LiNbO_3$; Xue & Zhang, 1997; Xue *et al.*, 2003), superconduction ($YBa_2Cu_3O_7$; Stahn *et al.*, 2005), colossal magnetoresistance ($La_{0.85}Ca_{0.15}MnO_3$; Lobanov *et al.*, 2000) *etc.* Therefore, it is desirable to search for the regularities governing whether perovskite compounds can be formed and the factors governing their structural stability, with the aim of providing useful clues for the discovery of novel materials.

The ionic-radii calculated tolerance factor (t_{IR}) was proposed to be a criterion of the structural stability of perovskite compounds (Goldschmidt, 1926)

$$t_{IR} = (R_A + R_O)/[2^{1/2} \times (R_B + R_O)]. \quad (1)$$

Here R_A, R_B and R_O represent the ionic radii of A and B cations, and the O anion for ABO_3-type compounds. In an ideal cubic perovskite structure, twice the B—O bond distance is equal to the unit-cell edge and twice the A—O bond distance is equal to the face diagonal of the unit cell. Therefore, if the bond distance is roughly assumed to be the sum of two ionic radii, the t_{IR} value of an ideal cubic perovskite should be equal to 1. However, experimental data indicated that t_{IR} values of most ideal cubic perovskite compounds were in the range 0.8–0.9, and distorted perovskite compounds (Goldschmidt, 1926) occurred with a wider range of t_{IR} values. Furthermore, the original formula of t_{IR} [see (1)] neglects the influence of coordination number on the effective ionic radii and some effective ionic radii of the required coordination number are unavailable, which leads to a different range of t_{IR} values (Goodenough *et al.*, 1972; Randall *et al.*, 1990; Eitel *et al.*, 2001). Thus, a uniform criterion for the structural stability of perovskite compounds cannot be obtained. In order to solve this problem, the ideal A—O and B—O bond distances (d_{A-O} and d_{B-O}) based on the BVM, which are substituted in place of the sum of the ionic radii, were applied to calculate the bond-valence-based tolerance factor (t_{BV}; Lufaso & Woodward, 2001), which is suggested as a new criterion of the structural stability of ABO_3-type perovskite compounds. Furthermore, one derivative of the BVM is the global instability index (GII), which can be used to estimate the structural stability of compounds. The structural stability of perovskite compounds composed of different atoms can be evaluated by its GII value, which is calculated using the ideal valence state of the B cation (Lufaso & Woodward, 2001). When we calculated the GII value, both bond distances and the oxidation states of cations and anions in the whole structure were comprehensively taken into account. In this regard the structural stability of ABO_3-type perovskite compounds can be well understood by the BVM.

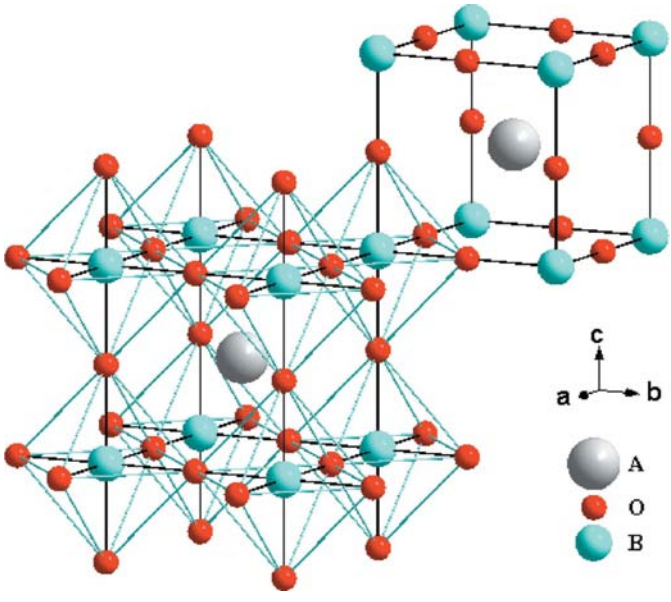

Figure 1
Fragment of the crystal structure of an ideal cubic perovskite. Note the corner-sharing BO_6 octahedra, extending in three dimensions to form the network.

Structure-map technology has attracted much attention since the 1950s. A two-dimensional graphic was proposed to study the stability of different compounds by Mooser and Pearson in 1959. The two parameters they applied were the electronegativity difference between the cation and the anion, and their average principle quantum number (Mooser & Pearson, 1959). Similar methods were termed structure-map technology and more parameters were used to draw the graphic. For example, a structure map to study the distribution of different structures for many ternary structural families was proposed by using the ionic radii of two cations (Muller & Roy, 1974). To predict the structure of $A^{3+}B^{3+}O_3$-type compounds, one structure map that relies on ionic radius and bond ionicity was attempted (Giaquinta & Loye, 1994). In addition, a pattern-recognition atomic parameter method was also used to study the regularities of the formability of perovskite compounds (Ye *et al.*, 2002). Regularities governing perovskite formability were recently investigated using an empirical structure-map method for a limited number of ABO_3-type compounds (Li *et al.*, 2004), however, the physical meaning of some parameters was not clear enough and more compounds should be further studied in this case. In this paper three new structure maps that rely on the ideal bond distance calculated by the BVM were constructed with the aim of extensively analyzing the formability of ABO_3-type perovskite compounds. In these maps the perovskite formation regions are shown clearly, which may help us design novel materials with a perovskite or perovskite-related structure.

2. Methodology

The BVM is one of the methods to interpret the bond distances observed, and also to predict expected values in crystal structures, on the basis of a modified Pauling's second rule. More importantly, the applications of the BVM are independent of compound type; nearly all ionic, covalent and metallic materials can be well studied by the BVM (Urusov, 2003). Therefore, this model is a useful tool to investigate the physical and chemical properties of crystals from the viewpoint of the chemical bond. Recently, part of our work has

successfully shown that the BVM can help us not only to study the defect structure and Curie temperature of $LiNbO_3$ crystals (Xue & He, 2006; Zhang & Xue, 2007), but also to analyze the bonding structure and systematic classification of borates (Yu & Xue, 2006; Yuan & Xue, 2007). For the BVM, all atoms are considered to be cations or anions according to the sign of their oxidation states. The empirical correlation of (2) is used to determine the bond valence s_{ij} of a chemical bond from its distance d_{ij}

$$s_{ij} = \exp\left(\frac{d_0 - d_{ij}}{B}\right), \tag{2}$$

where B is empirically determined, but can often be regarded as a universal constant with the value of 0.37 Å, and d_0 is the bond-valence parameter, the values of which have already been tabulated for most cation–anion pairs (Brown, 2006). The calculated valence $V_{i(\mathrm{cal})}$ is the sum of bond valences s_{ij} of each ion i

$$V_{i(\mathrm{cal})} = \sum_j s_{ij}. \tag{3}$$

For any compound, the sum of bond valences around any ion i is approximately equal to its oxidation state V_i. In practice, in any crystallographic structure the difference between oxidation state and bond-valence sum is minimized to optimize the corresponding structure. The value of the discrepancy factor D_i (Rao *et al.*, 1998) is a measure of the lattice strains present in the compounds

$$D_i = V_i - V_{i(\mathrm{cal})}. \tag{4}$$

Furthermore, the measurement of D_i over the whole crystal structure is referred to as the GII

$$\mathrm{GII} = \left\{\left[\sum_{i=1}^{N}(D_i^2)\right]/N\right\}^{1/2}, \tag{5}$$

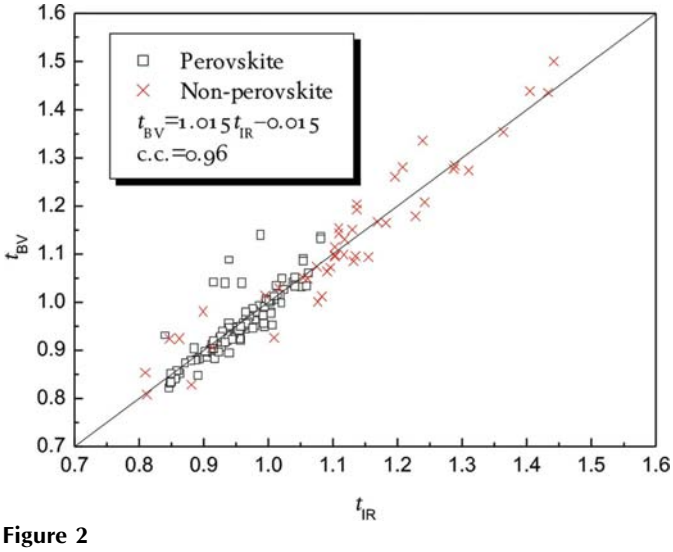

Figure 2
Correlation between ionic-radii calculated tolerance factors (t_{IR}) and bond-valence calculated tolerance factors (t_{BV}).

where N is the number of atoms in the formula unit. GII is a useful parameter to characterize the structural stability of compounds. Larger D_i and GII values indicate a strained bond that can lead to serious instabilities of crystal structure. To evaluate the structural stability of ABO_3-type perovskite compounds, GII are calculated using the ideal valence state of B cations, because the three-dimensional framework of corner-sharing BO_6 octahedra is the basic unit of the perovskite structure.

The ionic radii for a variety of coordination environments and oxidation states have been tabulated (Shannon, 1976). As shown in (1), the calculation of t_{IR} requires the A cation radius in 12-fold coordination sites, the B cation and the O anion radii in sixfold coordination sites. Unfortunately, 12-fold coordinate radii are not yet available for many cations and t_{IR} values cannot be obtained for many ABO_3-type compounds. In this regard the ideal A—O and B—O bond distances based on the BVM are currently employed to replace the sum of the ionic radii, assuming that 12 equidistant A—O bonds and six equidistant B—O bonds exist in the crystallographic frame. Therefore, (1) can be transformed into the following equation

$$t_{\mathrm{BV}} = d_{A-\mathrm{O}}/(2^{1/2} \times d_{B-\mathrm{O}}), \tag{6}$$

Substituting (2) and (3) into (6) and applying V_i instead of $V_{i(\mathrm{cal})}$, the following expression can be obtained

$$t_{\mathrm{BV}} = \frac{d_{0(A-\mathrm{O})} - B\ln(V_A/N_A)}{2^{1/2}[d_{0(B-\mathrm{O})} - B\ln(V_B/N_B)]}, \tag{7}$$

where V_A (V_B) is the oxidation state of the A (B) cation, and N_A (N_B) is the coordination number of the corresponding cation.

It should be noted that it is more reasonable to apply (8) to real crystals

$$t_{\mathrm{BV}} = \frac{d_{0(A-\mathrm{O})} - B\ln(\sum s_{ij(A)}/N_A)}{2^{1/2}[d_{0(B-\mathrm{O})} - B\ln(\sum s_{ij(B)}/N_B)]}. \tag{8}$$

However, (8) requires all individual s_{ij} values for a cation, which leads to a detailed calculation of all i—j bonds. In this work this case needs to become much simpler, *i.e.* by using V_i instead of Σs_{ij} (in this case our results t_{BV} can give a satisfactory agreement with t_{IR}, as shown in Fig. 2). Herein, (7) forms the basis of our calculation of t_{BV}.

The values of t_{BV} are calculated for 376 ABO_3-type compounds. For the stable structure of ABO_3-type perovskite compounds, the range of t_{BV} values can be obtained. On the basis of the ideal A—O and B–O bond distances, three two-dimensional structure maps are drawn to illuminate in more detail the likelihood of forming ABO_3-type perovskite compounds.

3. Results and discussion

3.1. Crystallographic data compiled

Data for all 376 ABO_3-type compounds were extracted for our study from the Inorganic Crystal Structure Database

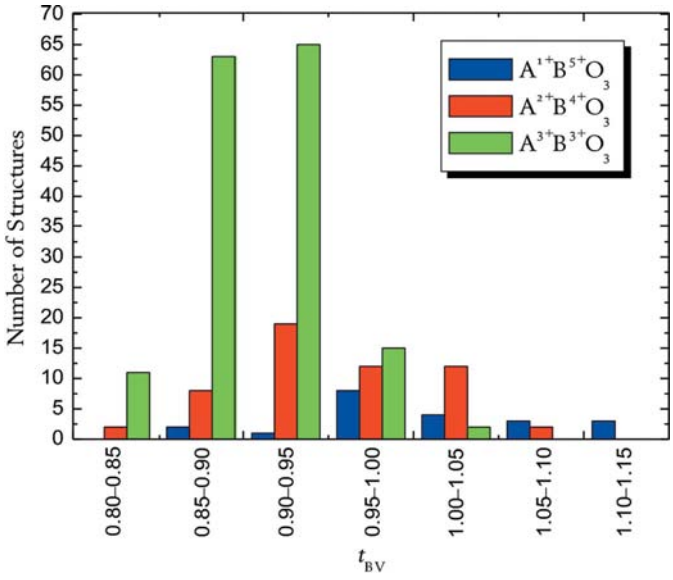

Figure 3
Distribution histogram of bond-valence based tolerance factors (t_{BV}) for ABO_3-type perovskite compounds.

(ICSD), Version 1.3.3 (2004), the Major Ternary Structural Families (Muller & Roy, 1974) and the most recent publications (Mizoguchi *et al.*, 2004; Ito *et al.*, 2001; Belik, Iikubo *et al.*, 2006; Belik, Stefanovich *et al.*, 2006; Belik, Wuernisha *et al.*, 2006). These compounds can be classified into three groups: $A^+B^{5+}O_3$-type, $A^{2+}B^{4+}O_3$-type and $A^{3+}B^{3+}O_3$-type. The ideal cubic perovskite can be transformed into other crystal structures through cation displacements and the simple tilting of BO_6 octahedra (Lufaso & Woodward, 2001). In general, there are 15 types of structures belonging to the perovskite catalog and each of them adopts a unique space-group symmetry. Therefore, the criteria for classifying an ABO_3-type perovskite compound is that it adopts one of the 15 crystal structures, its coordination number for the A cation must be in the range 8–12 and the coordination number for the B cation is 6. In addition, the influences of temperature and pressure on the ideal bond distances of ABO_3-type perovskite compounds are ignored in our study. All the 376 ABO_3-type compounds have been studied in this work. The results indicate that 232 ABO_3-type compounds (confirmed by Muller & Roy, 1974; Galasso, 1990; Rohrer, 2001; Mizoguchi *et al.*, 2004; Ito *et al.*, 2001; Belik, Iikubo *et al.*, 2006; Belik, Stefanovich *et al.*, 2006; Belik, Wuernisha *et al.*, 2006) belong to the perovskite structure, while the remaining compounds are non-perovskites. Of all the 376 ABO_3-type compounds, their ideal $A-O$ and $B-O$ bond distances (d_{A-O} and d_{B-O}), ionic-radii calculated tolerance factors (t_{IR} if possible), bond-valence calculated tolerance factors (t_{BV}) and GII values are listed in Table S1 (for $A^+B^{5+}O_3$-type), Table S2 (for $A^{2+}B^{4+}O_3$-type) and Table S3 (for $A^{3+}B^{3+}O_3$-type), respectively, of the supplementary material.[1]

[1] Supplementary data for this paper are available from the IUCr electronic archives (Reference: BS5049). Services for accessing these data are described at the back of the journal.

3.2. Structural stability of ABO_3-type perovskite compounds

The tolerance factors of 376 ABO_3-type compounds were calculated by the BVM and ionic-radii sum. The relationship between the t_{BV} and t_{IR} values obtained is shown in Fig. 2. The t_{BV} values vary from 0.822 to 1.139 for ABO_3-type perovskite compounds. The wider range of t_{BV} values may be caused by the increase in number of t_{BV} values. The linear correlation between t_{IR} and t_{BV} can be described by the equation $t_{BV} = 1.015t_{IR} - 0.015$, with the correlation coefficient 0.96. Some deviations from the linear dependence exist for five perovskite structural iodates, *i.e.* AIO_3 (A = Cs, Rb, K, Na and Tl), which may be ascribed to the larger difference between the ionic-radii sum of iodine and oxygen and the ideal I—O bond distance. Therefore, it is more reasonable to evaluate the tolerance factor by using the ideal bond distance rather than the ionic-radii sum. Simultaneously, a new geometric constraint for the stable perovskite structure is expected within the limit of t_{BV} values from 0.822 to 1.139. The distribution histogram of t_{BV} values for the 232 ABO_3-type perovskite compounds is shown in Fig. 3. It can be seen that for the different oxidation states of A and B (*i.e.* in $A^+B^{5+}O_3$-type, $A^{2+}B^{4+}O_3$-type, $A^{3+}B^{3+}O_3$-type perovskite compounds), the main distribution regions are different and the range of t_{BV} values is widened as the oxidation state of the B cation increases. Strictly speaking, t_{BV} values vary from 0.886 to 1.139 for $A^+B^{5+}O_3$-type perovskite compounds, from 0.822 to 1.061 for $A^{2+}B^{4+}O_3$-type compounds and from 0.832 to 1.012 for $A^{3+}B^{3+}O_3$-type compounds. Obviously, the number of ABO_3-type perovskite compounds sharply increases as the oxidation state of the B cation decreases.

The overall structural stability can be evaluated by the GII. The calculated GII values are compared with t_{BV} values for 232 ABO_3-type perovskite compounds, as shown in Fig. 4. It can be found that the GII values are close to 0 when t_{BV} values approach 1, and all GII values are less than 1.2 v.u. for ABO_3-

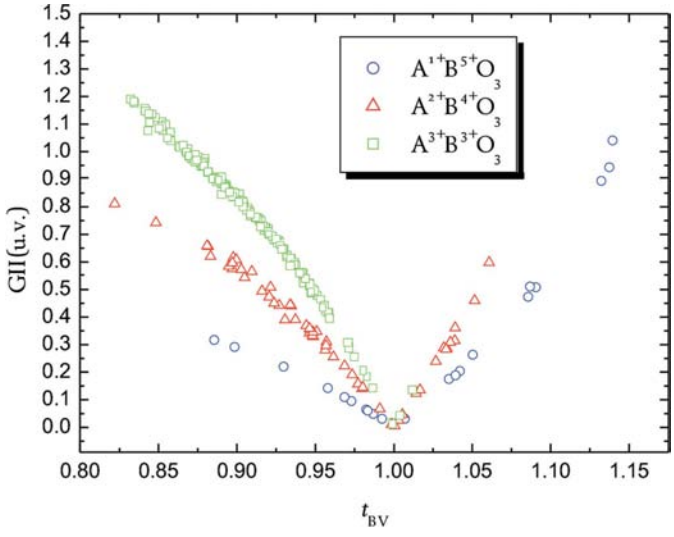

Figure 4
Global instability indices (GII) *versus* bond-valence based tolerance factors (t_{BV}) for ABO_3-type perovskite compounds.

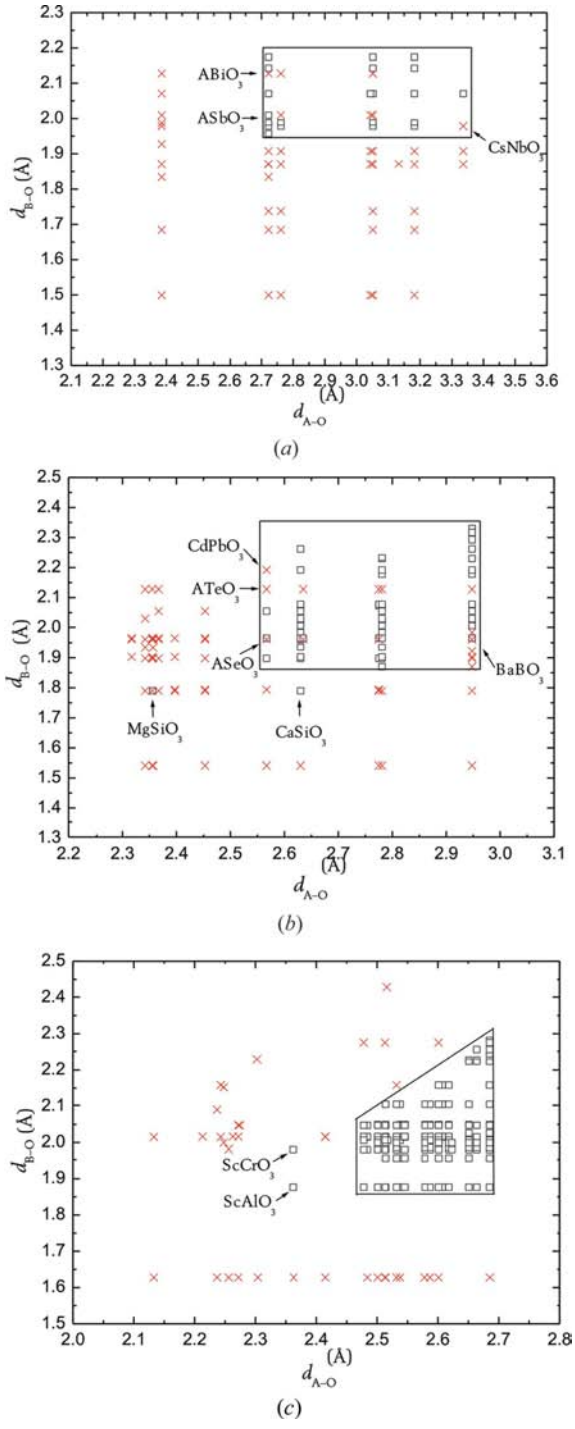

Figure 5
Structure maps plotted by the calculated ideal $A-O$ and $B-O$ bond distances (d_{A-O} and d_{B-O}) for ABO_3-type compounds (square symbols represent the perovskite structure and fork symbols represent the non-perovskite structure): (*a*) Perovskite formability of $A^+B^{5+}O_3$-type compounds (listed in Table S1 of the supplementary material for detailed information). $ABiO_3$ (A = Na, Ag and K) and $ASbO_3$ (A = Ag, K and Tl) represent the non-perovskite compounds; (*b*) perovskite formability of $A^{2+}B^{4+}O_3$-type compounds (listed in Table S2 of the supplementary material for detailed information). $ATeO_3$ (A = Cd, Hg, Pb, Sr and Ba), $ASeO_3$ (A = Cd, Hg and Pb) and $BaBO_3$ (B = Ru, Cr, Ge, Ni, Mn and Co) represent the non-perovskite compounds; (*c*) perovskite formability of $A^{3+}B^{3+}O_3$-type compounds (listed in Table S3 of the supplementary material for detailed information).

type perovskite compounds. In Fig. 4 it can also be seen that for the same t_{BV} value, GII values follow the sequence $A^{3+}B^{3+}O_3$-type > $A^{2+}B^{4+}O_3$-type > $A^+B^{5+}O_3$-type. The structural stability of ABO_3-type perovskite compounds follows the order $A^+B^{5+}O_3$-type > $A^{2+}B^{4+}O_3$-type > $A^{3+}B^{3+}O_3$-type, which is in good agreement with the analysis of real perovskite crystal structures.

3.3. Likelihood of forming of ABO_3-type perovskite compounds

Some ABO_3-type compounds exist that have t_{BV} values within the range 0.822–1.139; however, they exhibit non-perovskite structures. In order to further systemically analyze the likelihood of forming ABO_3-type perovskite compounds, we have plotted three structure maps for 64 $A^+B^{5+}O_3$-type, 119 $A^{2+}B^{4+}O_3$-type and 193 $A^{3+}B^{3+}O_3$-type compounds, respectively. As seen in Figs. 5(*a*)–(*c*), the horizontal and vertical axes represent the ideal $A-O$ and $B-O$ bond distances, respectively. It can be seen from Fig. 5(*a*) that the d_{A-O} values in the range 2.722–3.336 Å and the d_{B-O} values in the range 1.957–2.174 Å form the small rectangle region, which is defined as the empirical field of formation of $A^+B^{5+}O_3$-type perovskite compounds. In Fig. 5(*a*) the compounds located at the boundary region, such as $CsNbO_3$, have a non-perovskite structure as a result of the larger d_{A-O} values and the smaller d_{B-O} values. It can be observed that some antimonates and bismuthates do not have a perovskite structure in this rectangular region, on account of their stronger covalent Sb—O and Bi—O bonding interactions. However, it may also be possible for us to obtain the perovskite structure for such compounds by improving the synthesis methods and controlling the reaction conditions. For example, $NaSbO_3$ with a perovskite structure has been synthesized at 1273 K and 10 GPa in a uniaxial split-sphere anvil-type press (Mizoguchi *et al.*, 2004), which is the first ABO_3-type perovskite containing Sb^{5+} on the octahedral site. However, there is still an absence of perovskite structure compounds among ternary oxides of Bi^{5+}, which may also need extreme synthesis conditions.

As shown in Fig. 5(*b*), the d_{A-O} values are in the range 2.567–2.948 Å, the d_{B-O} values are in the range 1.870–2.330 Å, except those of $MgSiO_3$ and $CaSiO_3$. Therefore, the formation region of $A^{2+}B^{4+}O_3$-type perovskite compounds can be shown in this empirical rectangular field. In Fig. 5(*b*) some compounds located at the boundary region have a non-perovskite structure, such as $BaBO_3$ (B = Ru, Cr, Ge, Ni, Mn and Co). Since these compounds contain a B-type cation with larger electronegativity, BO_6 octahedra are more likely to be face-sharing than vertex-sharing, leading to hexagonal ABO_3-type structures, owing to the fact that in this case the effective electrostatic repulsion between B cations is relatively low because of the covalency of the $B-O$ bond (Muller & Roy, 1974). On the other hand, $CdPbO_3$, located at the boundary region, has a non-perovskite structure because of its smaller d_{A-O} and larger d_{B-O} values, both of which are a disadvantage in forming a perovskite structure. In addition, it is

observed that some selenates and tellurates have non-perovskite structures at the rectangular region of the formation of $A^{2+}B^{4+}O_3$-type perovskite compounds. A possible explanation is that the stability of the perovskite structure apparently decreases as the covalent interaction of the $B-O$ bond increases, while the strong covalent bonding inhibits the formation of 180° $B-O-B$ linkages (Mizoguchi *et al.*, 2004). In Fig. 5(*b*) $MgSiO_3$ (Vanpeteghem *et al.*, 2006) and $CaSiO_3$ (Magyari-Kope *et al.*, 2002) are not located at the rectangular region; however, both of them can form perovskite structures at high pressure. Therefore, it can be predicted that when the $A-O$ and $B-O$ ideal bond distances are smaller than their lower limits of the rectangular region with t_{BV} values of 0.822–1.139, a perovskite structure can also be formed by suitably controlling the synthesis conditions.

From Fig. 5(*c*), it is apparent that the d_{A-O} values are in the range 2.478–2.685 Å and the d_{B-O} values are in the range 1.876–2.281 Å, except those of $ScAlO_3$ and $ScCrO_3$. All of the $A^{3+}B^{3+}O_3$-type perovskite compounds (except $ScAlO_3$ and $ScCrO_3$) are perfectly distributed in the trapezoid region. It can be seen that larger d_{A-O} and smaller d_{B-O} values are advantageous for forming $A^{3+}B^{3+}O_3$-type perovskite compounds, while the smaller d_{A-O} and the larger d_{B-O} are disadvantageous. However, under high temperature and high pressure, the compounds with smaller d_{A-O} and d_{B-O} values can form a perovskite structure such as $ScAlO_3$ (Ross, 1998) and $ScCrO_3$ (Park & Parise, 1997). Recently, three new $A^{3+}B^{3+}O_3$-type perovskite compounds, $BiInO_3$, $BiAlO_3$ and $BiScO_3$ (Belik, Iikubo *et al.*, 2006; Belik, Stefanovich *et al.*, 2006; Belik, Wuernisha *et al.*, 2006), have been synthesized under high-pressure and high-temperature conditions. It was found that they fit well into the middle of the trapezoid region in the formation of $A^{3+}B^{3+}O_3$-type perovskite compounds. In summary, it should be noted that all of the non-perovskite compounds which appear in the perovskite formation regions will possibly convert to perovskite compounds under special conditions, suggesting numerous opportunities and challenges for synthetic chemists. Moreover, this indicates that the likelihood of forming ABO_3-type perovskite compounds is mainly determined by the $A-O$ and $B-O$ bond distances and t_{BV} values, while temperature and pressure can enlarge the perovskite formation region.

4. Conclusions

In this work 376 ABO_3-type compounds, including $A^{+}B^{5+}O_3$-type, $A^{2+}B^{4+}O_3$-type and $A^{3+}B^{3+}O_3$-type compounds, were investigated; of which, only 232 ABO_3-type compounds have a perovskite structure. By applying the BVM to these 376 compounds, the t_{BV} values for ABO_3-type perovskite compounds were found in the range 0.822–1.139, which can be regarded as a new criterion for the structural stability of ABO_3-type perovskite compounds. The overall structural stability has been evaluated by the GII that was calculated using the ideal valence state of the *B* cation. Furthermore, GII values were found to be less than 1.2 v.u. and they increase with a decrease of oxidation state of the *B* cations. The structural stability of ABO_3-type perovskite compounds was found to follow the order $A^{+}B^{5+}O_3$-type > $A^{2+}B^{4+}O_3$-type > $A^{3+}B^{3+}O_3$-type compounds. The formability regularities of ABO_3-type perovskite compounds were investigated by three two-dimensional structure maps, which were plotted using the ideal $A-O$ and $B-O$ bond distances. The sample points representing compounds of the perovskite and non-perovskite structure are distributed in different regions. Provided that the proper synthetic techniques are employed, we suggest that some non-perovskite compounds located at the perovskite formation region may possibly be crystallized in a perovskite structure. Therefore, the utility of the structure-map technology lies not only on rationalizing the structure of known compositions, but also on predicting the structure of novel compositions. Furthermore, the current method is also applicable to materials with anions other than oxygen, *e.g.* nitrides, chalcogenides or halides.

This work was supported by the program for New Century Excellent Talents in University (NCET-05-0278); the National Natural Science Foundation of China (Grant No. 20471012), a Foundation for the Author of National Excellent Doctoral Dissertation of People's Republic of China (Grant No. 200322), the Research Fund for the Doctoral Program of Higher Education (Grant No. 20040141004), and the Scientific Research Foundation for the Returned Overseas Chinese Scholars, State Education Ministry.

References

Alekseeva, A. M., Abakumov, A. M., Rozova, M. G., Antipov, E. V. & Hadermann, J. (2004). *J. Solid State Chem.* **177**, 731–738.
Belik, A. A., Iikubo, S., Kodama, K., Igawa, N., Shamoto, S., Maie, M., Nagai, T., Matsui, Y., Stefanovich, Y. S., Lazoryak, B. I. & Takayama-Muromachi, E. (2006). *J. Am. Chem. Soc.* **128**, 706–707.
Belik, A. A., Stefanovich, S. Y., Lazoryak, B. I. & Takayama-Muromachi, E. (2006). *Chem. Mater.* **18**, 1964–1968.
Belik, A. A., Wuernisha, T., Kamiyama, T., Mori, K., Maie, M., Nagai, T., Matsui, Y. & Takayama-Muromachi, E. (2006). *Chem. Mater.* **18**, 133–139.
Brown, I. D. (2006). http://www.ccp14.ac.uk/ccp/web-mirrors/i_d_brown.
De, P. A. & Barresi, A. A. (2001). *Ind. Eng. Chem. Res.* **40**, 1460–1464.
Eitel, R. E., Randall, C. A., Shrout, T. R., Rehrig, P. W., Hackenberger, W. & Park, S. E. (2001). *Jpn. J. Appl. Phys.* **40**, 5999–6002.
Galasso, F. S. (1990). *Perovskites and High Tc Superconductors.* New York: Gordon and Breach Science Publishers.
Giaquinta, D. M. & Loye, H. C. (1994). *Chem. Mater.* **6**, 365–372.
Goldschmidt, V. M. (1926). *Naturwissenschaften*, **14**, 477–485.
Goodenough, J. B., Kafalas, J. A. & Longo, J. M. (1972). *Preparative Methods in Solid State Chemistry*, edited by P. Hagenmuller. New York: Academic Press.
Ito, K., Tezuka, K. & Hinatsu, Y. (2001). *J. Solid State Chem.* **157**, 173–179.
Kajitani, M., Matsuda, M., Hoshikawa, A., Harjo, S., Kamiyama, T., Ishigaki, T., Izumi, F. & Miyake, M. (2005). *Chem. Mater.* **17**, 4235–4243.
Khalyavin, D. D., Salak, A. N., Vyshatko, N. P., Lopes, A. B., Olekhnovich, N. M., Pushkarev, A. V., Maroz, I. I. & Radyush, Y. V. (2006). *Chem. Mater.* **18**, 5104–5110.
Li, C., Soh, K. C. K. & Wu, P. (2004). *J. Alloys Compd.* **372**, 40–48.

Lobanov, M. V., Balagurov, A. M., Pomjakushin, V. J., Fischer, P., Gutmann, M., Abakumov, A. M., D'yachenko, O. G., Antipov, E. V., Lebedev, O. I. & Tendeloo, G. V. (2000). *Phys. Rev. B*, **61**, 8941.
Lufaso, M. W. & Woodward, P. M. (2001). *Acta Cryst.* B**57**, 725–738.
Magyari-Kope, B., Vitos, L., Grimvall, G., Johansson, B. & Kollar, J. (2002). *Phys. Rev. B*, **65**, 193107.
Mizoguchi, H., Woodward, P. M., Byeon, S. H. & Parise, J. B. (2004). *J. Am. Chem. Soc.* **126**, 3175–3184.
Mooser, E. & Pearson, W. B. (1959). *Acta Cryst.* **12**, 1015–1022.
Muller, O. & Roy, R. (1974). *The Major Ternary Structural Families.* Berlin, Heidelberg, New York: Springer-Verlag.
Park, J. H. & Parise, J. B. (1997). *Mater. Res. Bull.* **32**, 1617–1624.
Randall, C. A., Bhalla, A. S., Shrout, T. R. & Cross, L. E. (1990). *J. Mater. Res.* **5**, 829–834.
Rao, G. H., Barner, K. & Brown, I. D. (1998). *J. Phys. Condens. Matter*, **10**, 757–763.
Rohrer, G. S. (2001). *Structure and Bonding in Crystalline Materials.* Cambridge University Press.
Rooke, J. & Weller, M. (2003). *Solid State Phenom.* **90**, 417–422.
Ross, N. L. (1998). *Phys. Chem. Miner.* **25**, 597–602.
Sato, T., Noreus, D., Takeshita, H. & Haussermann, U. (2005). *J. Solid State Chem.* **178**, 3381–3388.
Shannon, R. D. (1976). *Acta Cryst.* A**32**, 751–767.
Stahn, J., Chakhalian, J., Niedermayer, C., Hoppler, J., Gutberlet, T., Voigt, J., Treubel, F., Habermeier, H. U., Cristiani, G., Keimer, B. & Bernhard, C. (2005). *Phys. Rev. B*, **71**, 140509.
Suchomel, M. R., Fogg, A. M., Allix, M., Niu, H., Claridge, J. B. & Rosseinsky, M. J. (2006). *Chem. Mater.* **18**, 4987–4989.
Urusov, V. S. (2003). *Z. Kristallogr.* **218**, 709–719.
Vanpeteghem, C. B., Zhao, J., Angel, R. J., Ross, N. L. & Bolfan-Casanova, N. (2006). *Geophys. Res. Lett.* **33**, 03306.
Xue, D. & He, X. (2006). *Phys. Rev. B*, **73**, 064113.
Xue, D., Wu, S., Zhu, Y., Kazuya, T., Kenji, K. & Wang, J. (2003). *Chem. Phys. Lett.* **377**, 475–480.
Xue, D. & Zhang, S. (1997). *J. Phys. Condens. Matter*, **9**, 7515–7522.
Ye, C. Z., Yang, J., Yao, L. X. & Chen, N. Y. (2002). *Chin. Sci. Bull.* **47**, 458–460.
Yu, D. & Xue, D. (2006). *Acta Cryst.* B**62**, 702–709.
Yuan, G. & Xue, D. (2007). *Acta Cryst.* B**63**, 353–362.
Zhang, X. & Xue, D. (2007). *J. Phys. Chem. B*, **111**, 2587–2590.